# Shielding and activation studies for the design of the MYRRHA proton beamline

**Anna Ferrari[1], Jean-Luc Biarrotte[2],**
**Luc Perrot[2], Hervé Saugnac[2], Dirk VandePlassche[3]**
[1]Institute of Radiation Physics, Dresden, Germany
[2]CNRS-IN2P3, Université Paris Sud, IPNO, Orsay, France
[3]SCK·CEN, Mol, Belgium

## Abstract

*Accelerator-driven systems require the use of high energy Mega-Watt proton beams, in combination with a nuclear reactor core operating in subcritical mode. Between the challenges in the design, key points are the radiation shielding and the minimisation of the induced activation. The present study has been done to optimise the design of the MYRRHA facility at SCK•CEN in Mol (Belgium), where a 600 MeV, 4 mA proton beam will be produced and transported through a linear accelerator up to a LBE spallation target, located inside the core of a LBE-cooled reactor, operating at 94 MW when coupled with the proton accelerator. To assess some aspects of the shielding of the proton beamline, as well as to fix the activation problems that heavily influence the design, extensive simulations have been performed with the FLUKA Monte Carlo code. In the first part of this work a systematic study has been finalised to estimate the neutron production and the radioactivity induced by the MYRRHA proton beam in typical materials used in the accelerator structures. The results of this study allow optimising the design of the elements devoted to the total or partial beam absorption (beam dump, collimators). It will be shown, in particular, how a suitable material configuration can improve the accessibility and the long-term treatment of the irradiated elements.*

## Introduction

Accelerator-driven systems (ADS) are one of the options studied for the transmutation of nuclear waste in the European Community. With the aim of demonstrating efficient transmutation of high-level waste and associated ADS technology, the FP7 European project Central Design Team (CDT) has worked from 2009 to 2012 to design the FAst Spectrum Transmutation Experimental Facility (FASTEF), on which the MYRRHA research facility [1] at SCK·CEN in Mol (Belgium) will be based. The heart of the system is a lead-bismuth eutectic (LBE)-cooled reactor, working both in critical and in sub-critical operation modes. The neutrons needed to sustain fission in the subcritical mode are produced via spallation processes by a 600 MeV, 4 mA proton beam, which is provided by a linear accelerator and hits a LBE spallation target located inside the reactor core (see Figure 1). The use of high energy/high current proton beams itself presents many challenges for various aspects of the design, as already pointed out in the SATIF-10 Workshop [2]. The combination with a nuclear reactor core operating in subcritical mode with 94 MW power, or in critical mode with 100 MW power when not coupled with the proton beam, makes the shielding problem an issue: thick shielding for the prompt radiation, high target/dump activation, spent beam handling are the main points. Figure 1 shows that the general problem of the radiation containment can be divided into two parts: the shielding of the accelerator tunnel and the shielding of the reactor building. The present work focuses on the first problem, while the second one, still under investigation, has been treated elsewhere (for example in [3]). Two main points will be analysed as follows: the shielding and the activation of the element devoted to the full beam absorption (beam dump), and the activation of the materials, along the beam-line, where beam losses occur. To address these problems, an extensive simulation analysis with the FLUKA Monte Carlo code [4] [5] has been performed, as shown in the next two sections.

## Double differential neutron yields, residual dose rates and specific activities from irradiated thick reference materials

As a first step, a systematic study has been finalised to estimate the neutron production and the radioactivity induced by a proton beam – with the energy and the current foreseen at MYRRHA – in five typical materials used in the accelerator structures: carbon (a candidate material for the core structure of the dump); stainless steel (used in pipe, magnets and eventually as a part of the dump structure around the carbon core); copper (possible solution for the dump, but also present in magnet coils and cavities); aluminium (foreseen in some points of the beam-line instead of the stainless steel); iron (alternative material in the dump structure around the carbon core). This study, which aims to represent a natural extension of the work presented at the SATIF-10 Workshop [6] from lower proton energies up to the MYRRHA energy range, is intended to provide a simple database, useful to drive the choice of the main structural materials and to assess an approximate estimate of the radiological risk to be expected when interventions on the accelerator components are needed.

All the simulations have been carried out with the FLUKA Monte Carlo code, version 2011.2. A precious advantage of FLUKA is the possibility to evaluate, in the same simulation, not only the particle fluences and the ambient dose equivalent, H*(10), due to all the components of the prompt radiation field, but also the time evolution of the activation products and the transport of their emitted radiation.

**Figure 1: Layout of the last part of the FASTEF-MYRRHA proton beamline, until the spallation target inside the reactor core**

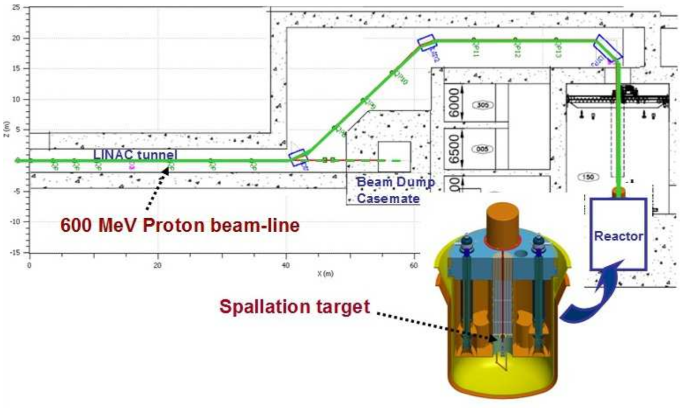


Given an irradiation pattern, the time evolution of the system (the time dependency of the isotopic densities, $N_i$, in the irradiated material) is evaluated run-time via the exact analytical solution of the Bateman equations, for which a particle fluence rate, $\varphi(E)$, constant during each considered time interval can be written as:

$$\frac{dN_i}{dt} = -\sum_{j \neq i}\left[\lambda_{ji}^{d} + \bar{\sigma}_{ji}\bar{\varphi}\right]N_i + \sum_{j \neq i}\left[\lambda_{ij}^{d} + \bar{\sigma}_{ij}\bar{\varphi}\right]N_j \quad (1)$$

where $\lambda^d_{ji}$ is the decay probability of the radionuclide i in the radionuclide j and $\sigma_{ji}$ is the particle induced cross-section for transmutation from the isotope i to the isotope j, and where the average spectrum, $\bar{\varphi}$, and the spectrum averaged, particle induced cross-section, $\bar{\sigma}_{ji}$, have been introduced:

$$\bar{\varphi} = \int \varphi(E)dE \qquad \bar{\sigma}_{ji} = \frac{1}{\bar{\varphi}}\int \varphi(E)\sigma_{ji}(E)dE \quad (2)$$

In Equation (1) the number of isotopes of species i decayed in other isotope species or transmuted via a nuclear reaction with the incoming beam, and the number of isotopes i produced via the decay of other radionuclides or via nuclear reactions are therefore taken into account.

At the same time FLUKA can perform the generation and transport of the residual radiation (in the used version of the code extended to γ, β+, β-, X-rays and conversion electron emissions). This means that in the same run we can obtain the production of the residuals, their time evolution and the residual dose due to their decay.

### *Double differential neutron yields*

First, we want to evaluate the neutron yield during the operation and the residual dose in the points where the beam can be completely absorbed (also with the goal to study suitable materials for the beam dump optimisation), so that the geometry structure of the irradiated materials has been considered as a thick target: for each sample a cylindrical structure has been chosen, with the height slightly exceeding the corresponding proton range (by a factor 1.2), the diameter equal to its height and the center of the coordinate system located at the center of the upstream face (in Table 1 the values are reported). A 600 MeV proton pencil beam, with a 4 mA current (2.497 $10^{16}$ p/s) has been simulated, hitting the center of the cylinder and directed along the z axis. The double differential yields of neutrons escaping from the target have been calculated in six angular bins with respect to the axis of the impinging proton beam: 0°-15°, 15°-45°, 45°-75°, 75°-105°, 105°-135° and 135°-180°. Figures 2 and 3 show the neutron spectra for carbon, AISI-316L and copper, together with a picture of the neutron fluence in and around the target in the case of carbon. The high energy spallation peak, which decreases at large angles and is strongly suppressed in the backward direction, is well visible in all cases. The evaporation peak at around 1 MeV is important (in terms of neutron yield) in the high-Z materials, and in the neutron distributions of stainless steel is also clearly visible the resonance structure, mainly due to the iron component. The neutron distributions from the carbon target show the typical moderation peak. In Table 2 the total neutron yields and the yields for the very forward (0°-15°) and backward (135°-180°) components of the radiation are summarised. They give a first quantitative indication about the advantage in using soft materials (carbon) as main components of the structures that are directly hit by the proton beam.

**Table 1: Dimensions and densities of the sample targets**

| | Sample height (cm) | Sample radius (cm) | Material density ($g/cm^3$) |
|---|---|---|---|
| Carbon | 105 | 52.5 | 2.0 |
| Copper | 30.5 | 15.25 | 8.98 |
| AISI-316L | 35 | 17.5 | 8.0 |
| Aluminium | 87.5 | 43.75 | 2.70 |
| Iron | 35 | 17.5 | 7.87 |

***Residual dose rates***

The analysis of the dose rates due to the residual radiation and of the activation products has been performed on the same samples by studying two irradiation patterns. A short-term irradiation has been simulated in the most conservative beam conditions during the commissioning: 24 hours continuous operation at the maximum beam energy and intensity. Cooling times have been analysed between the end of irradiation (EOI) and the following 24 hours. Moreover, a long-term irradiation has been simulated by considering 2 years of commissioning and 5 years of normal operation and adopting the scheme, motivated by the need to operate also in critical mode, of 1 months of operation at 6 hours/day followed by 3 months of stop, considered as a continuous time interval. Cooling times have been analysed, in this case, until one year after the EOI. The ambient dose equivalent rates due to the residual radiation around the samples are shown in Figures 4 and 5 for copper and carbon in the case of short-term irradiations. We observe that for the copper, as well as for the AISI-316L sample, the residual dose rates are very high (at the level of some tens of Sv/h) already after short irradiations and considering a reasonable cooling time of 24 hours. In Figure 6 the evolution of the H*(10) at 50 cm from the front side of the target is reported as a function of the cooling time, for both the irradiation patterns and for the samples in copper, carbon and stainless steel. We can observe that the high-Z materials exhibit very high dose rates also after long cooling times: in particular the activated radionuclides in copper still give around 20 Sv/h after 5 years from the end of the long-term irradiation. This analysis suggests the use of innovative, combined solutions, with soft (low-Z) materials inserted, where possible, in the parts of the accelerator that are directly hit by the full beam, as is the case of the beam dump.

**Figure 2: Neutron double differential spectra from the target in carbon (left) and neutron fluence in and around the same sample (right)**

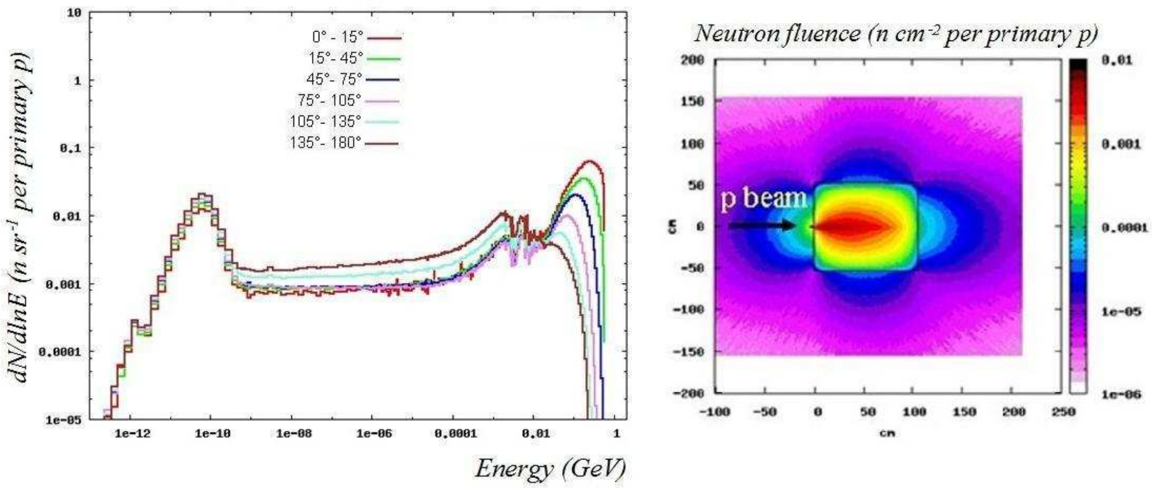


**Figure 3: Neutron double differential spectra from the targets in stainless steel (left) and in copper (right)**

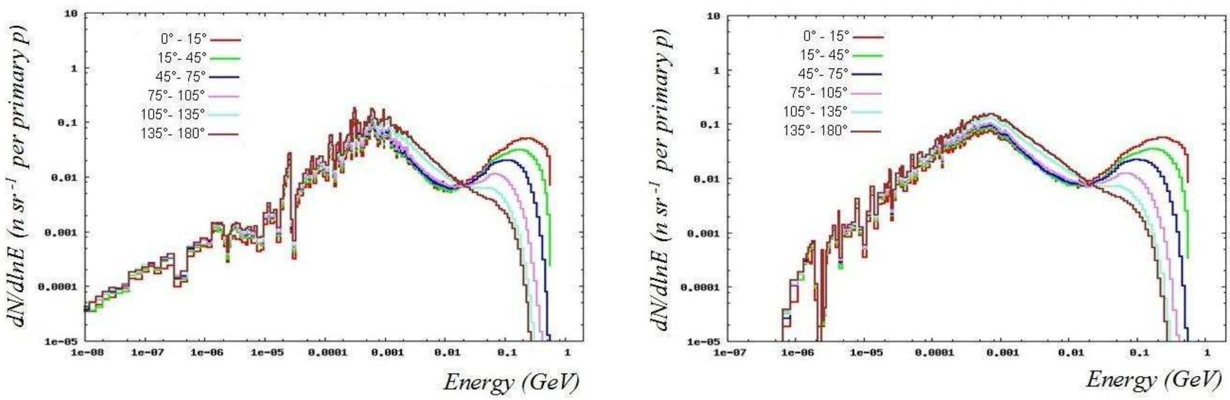


**Table 2: Neutron yields computed for the sample targets**

| | Neutron yield (n/p) | | | | | |
|---|---|---|---|---|---|---|
| | Forward direction (0°-15°) | | Backward direction (135°-180°) | | Total | |
| | Full energy spectrum | $E_n$>100 keV | Full energy spectrum | $E_n$>100 keV | Full energy spectrum | $E_n$>100 keV |
| Carbon | 0.036 | 0.029 | 0.190 | 0.068 | 1.195 | 0.554 |
| Copper | 0.067 | 0.062 | 0.747 | 0.684 | 3.989 | 3.625 |
| AISI-316L | 0.055 | 0.052 | 0.619 | 0.569 | 3.308 | 3.021 |
| Iron | 0.059 | 0.056 | 0.663 | 0.585 | 3.478 | 3.215 |
| Aluminium | 0.048 | 0.038 | 0.376 | 0.261 | 2.161 | 1.439 |

Note: The values in the region of the neutron energy spectrum > 100 keV are also reported.

### *Specific activities*

As a last step, the specific activity of the irradiated samples has been evaluated, putting in evidence the contribution of the single radionuclides. In all of the Monte Carlo calculations the statistical error has been kept at the level of few percent. In Figures 7 and 8 the radionuclide composition of the activated samples is shown in the copper and in the carbon case, for short-and long-term-irradiations. In the copper case a total specific activity of 2.27 $10^{11}$ Bq/cm$^3$ is evaluated after 24 hours irradiation and 8 hours cooling, the main contributors (also under the point of view of radiological importance) being? the cobalt products as $^{56}$Co, $^{57}$Co, $^{58}$Co and $^{60}$Co. After a long-term irradiation and 10 years cooling the copper sample still exhibits a total specific activity of 1.2 $10^{10}$ Bq/cm$^3$, mainly due to long-life radionuclides like $^{60}$Co ($t_{1/2}$=5.27 years), which is the dominant isotope, $^{63}$Ni ($t_{1/2}$=100.1 years) and $^{55}$Fe ($t_{1/2}$=2.737 years). The graphite sample shows a specific activity of 4.0 $10^7$ Bq/cm$^3$ after 24 hours irradiation and 8 hours cooling, mainly due to the $^7$Be and tritium contributors. After a long-term irradiation and 10 years cooling the carbon total specific activity is at the level of 4.1 $10^8$ Bq/cm$^3$ and is completely dominated by tritium. The results for the stainless steel sample in the case of a long-term irradiation are shown in Figure 9, where the behaviour of all contributors is shown for cooling times up to 5 years: the total specific activity is around 8 $10^{10}$ Bq/cm$^3$ and is dominated by $^{55}$Fe. It must be stressed, however, that in the present calculation the sample of AISI-316L has been simulated in the ideal situation where cobalt impurities are not present: such impurities have to be foreseen and they should be maintained at the lowest reasonable level (typical values are fractions of 0.1-0.5 per-mille in volume).

**Figure 4: H*(10) Residual dose rate around the copper target, at different cooling times after a 24 h irradiation**

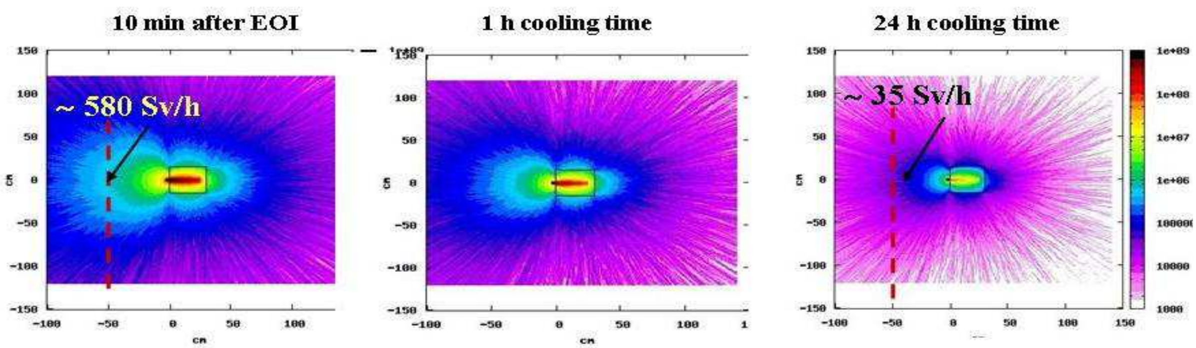


**Figure 5: H*(10) Residual dose rate around the carbon target, at different cooling times after a 24 h irradiation**

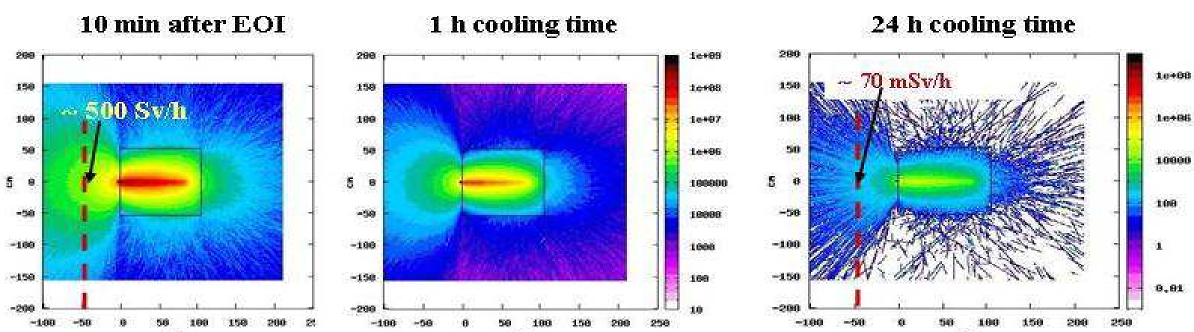

**Figure 6: H*(10) Residual dose rate evaluated at 50 cm from the front of the target samples as a function of the cooling time, for short-(left) and long-term (right) irradiations**

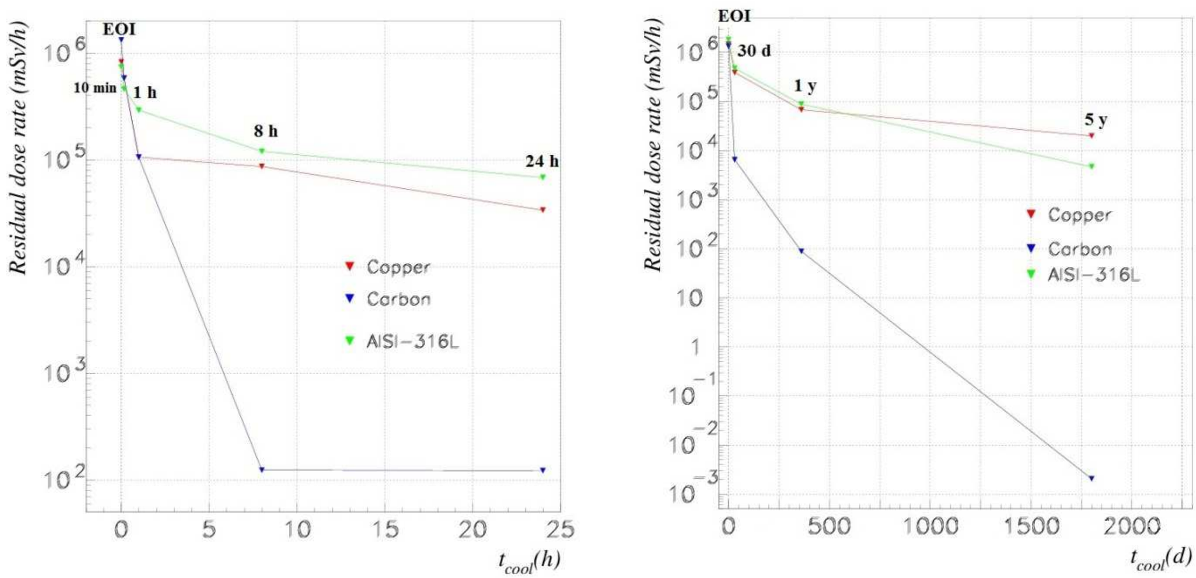


**Figure 7: Specific activity (in Bq/cm³) of the copper and carbon samples in the case of short-term irradiation, after 8 hours cooling**

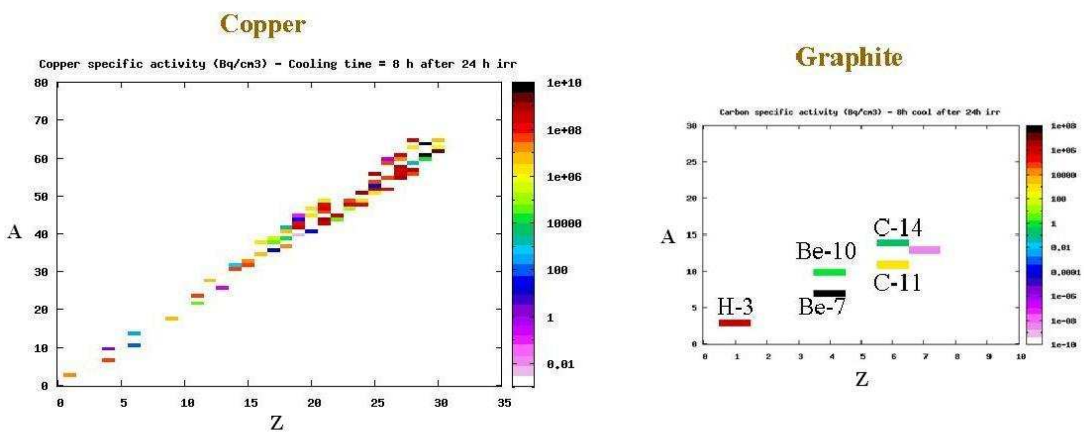


It is represented in the Z-A plane to show the contribution of the single radionuclides.

**Figure 8: Specific activity (in Bq/cm³) of the residual radionuclides evaluated in the samples of copper and carbon in the case of a long-term irradiation, after 10 year cooling**

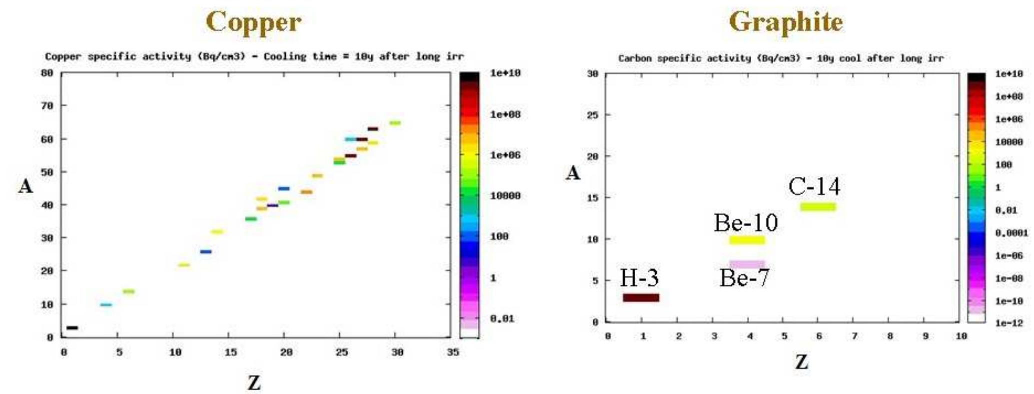


**Figure 9: Behaviour of the total specific activity (in Bq/g) of the stainless steel sample in the case of the long-term irradiation, for different cooling times up to 5 years**

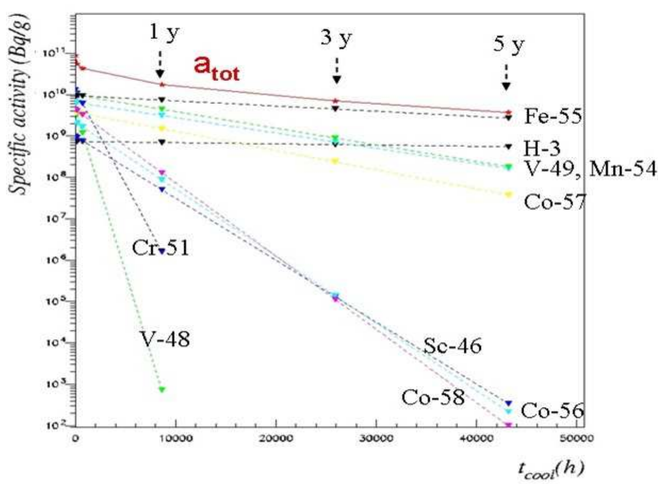


The contribution of the main radionuclides is reported.

## Optimisation study of the beam dump

The beam dump will always absorb the beam completely during the period of the accelerator commissioning, and for accelerator tuning purposes during the operation time. It will be, therefore, the “hottest” part of the accelerator beam-line. The first solution thought for the beam dump is based on the model adopted at PSI for the High Intensity Proton Accelerator Facility [7], because the beam characteristics (590 MeV proton beam energy and maximum beam current of 2 mA, corresponding to a full power of 1.2 MW) are very close to the MYRRHA requirements. The PSI beam dump is composed of 4 copper blocks (see Figure 10), cooled with water and placed in a parallelepiped-shaped vacuum chamber. Each copper block extends to a stainless steel block, ~3 m long. A preliminary upgrade of the PSI solution has been evaluated to fit the MYRRHA requirements and foresees the use of 5-6 copper elements. This solution, which presents the advantage of a consolidated know-how, does not exhibit, however, the best performances under the point of view of the radiation protection. As it can be argued from the studies presented in the previous section, with this solution quite a high-yield of secondary neutrons and serious activation problems are to be expected. For this reason two approaches have been followed in parallel: to quantify and possibly to limit the main problems in the copper dump design and, on the other hand, to propose and to explore an alternative solution. This one has been identified in a bi-material structure, with a suitable soft material as dump core, surrounded by a high-Z shielding structure. As already pointed out elsewhere [8] [9], advantages of this concept are a smaller neutron yield, an energy deposition over a wider range and consequently considerable less activation problems, especially in terms of residual ambient dose equivalent rate. A key point that drives the choice in favour of a soft material core is that in this case the build-up region of the secondary radiation moves from the front part towards the central part of the dump, with a very effective auto-shielding effect: the "hottest" part of the dump is not anymore close to the dump surface but is deeper inside the material, minimising the H*(10) rate outside the dump.

**Figure 10: The PSI 1.2 MW beam dump**

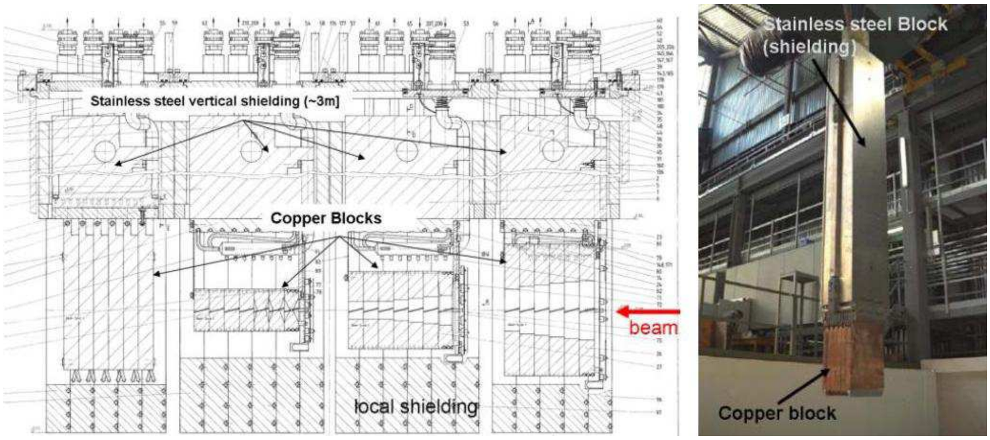


**Figure 11: The FASTEF-MYRRHA beam dump casemate along the proton beamline**

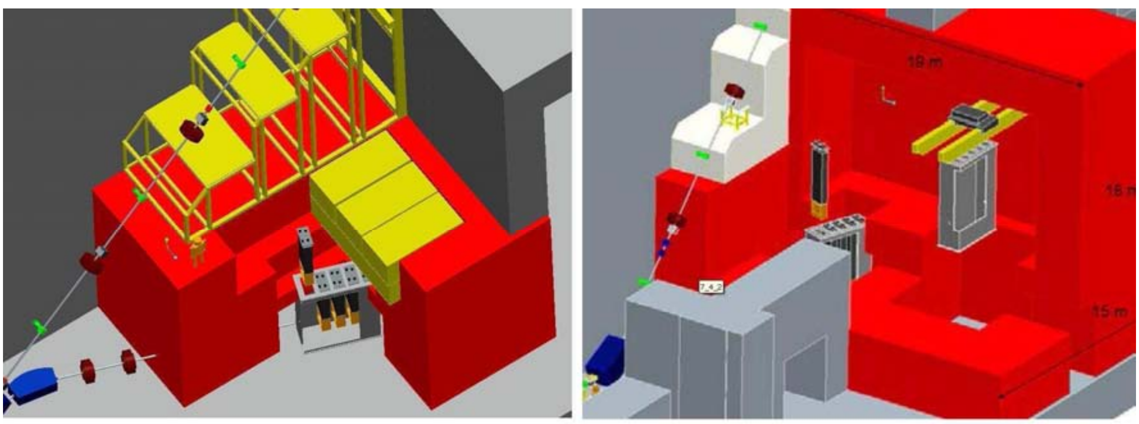

Left: the simulated design of the irradiated cell. Right: a possible design with a second cell for maintenance and a crane for remote handling.

A bi-material solution in carbon (graphite for shielding, with a density of ~ 2.0 g/cm$^3$) and stainless steel (AISI-316L) has been studied. The dimensions assumed for the carbon core are 50 cm in radius and 180 cm in length, while for the high-Z part a radius of 140 cm and a length of 330 cm have been set. The model implemented in FLUKA also includes the whole concrete cage, with walls ~5 m thick, and the last part of the proton beam-line. Parallel simulations of a complete model of the beam dump in copper, with 5 copper elements and their extensions in stainless steel, have been also performed. Figure 12 shows a comparison between the two models in terms of neutron fluence. Firstly, it should be stressed that the casemate in concrete contains the radiation in a very satisfactory way in both cases. The average neutron fluence inside the concrete cage, however, is in the bi-material case ~100 times lower. Moreover, if the neutron secondary radiation emitted in the backward direction is studied (see Figure 13), it can be observed that the bi-material solution minimises the part of the spectrum from the epithermal up to the fast and the high energy neutrons. This result is also more interesting if in this sample the neutrons that pass through the pipe channel and come out from the shielding wall are selected: the spectra of these neutrons (in red in Figure 13) show that the backscattered neutron radiation reaching the beamline is bigger in the copper case and is never negligible. For this reason, with the aim of protecting the instrumentation close to the dipole at 45° positioned at the beginning of the vertical beamline, together with the horizontal beam tube before, the portion of the proton line between this dipole and the dump has been rotated of 20° with respect to the horizontal beamline, as illustrated in Figure 11.

**Figure 12: Neutron fluence (n/cm$^2$ per primary proton) in the dump concrete cage in the case of the dump in copper (left) and of the bi-material dump in carbon and stainless steel (right)**

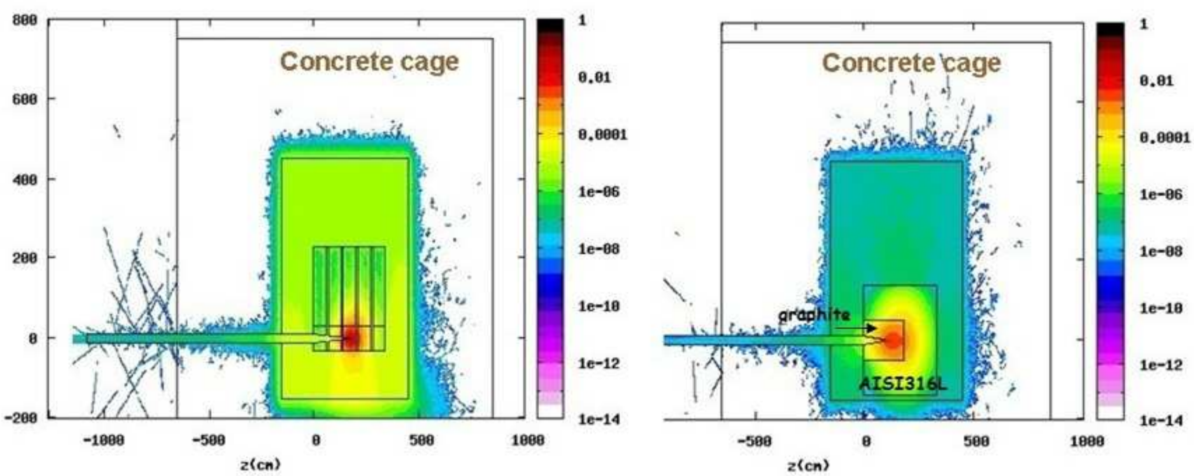

**Figure 13: Spectra of the neutrons (neutrons $sr^{-1}$ per primary proton) coming out from the dump in the backward direction, for the two studied models of the beam dump**

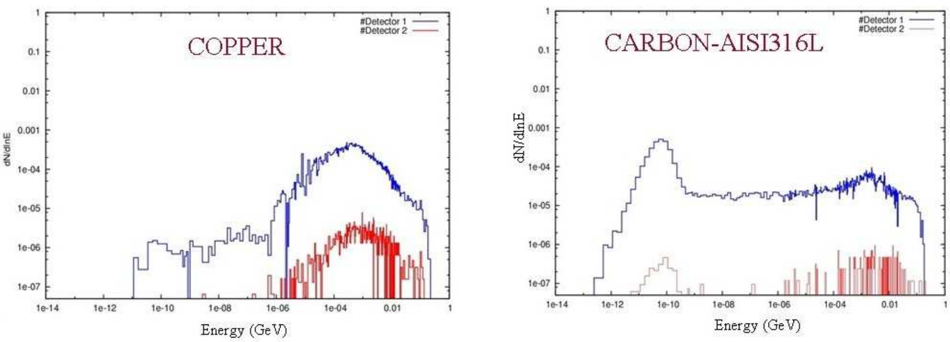


In blue all the backward neutrons from the copper structure (left) and from the graphite/stainless steel structure (right) are computed. In red, the neutrons are reported that, going in the backward direction, cross the shielding walls along the beam-line tunnel and reach the accelerator hall.

### *Residual dose rates and specific activities*

A special study has been dedicated to the evaluation of the residual dose rates expected inside the concrete cage and on the roof for the two models of the beam dump. The special capability of the FLUKA code has been used to perform a simulation in a condition of variable geometry: the geometry of the problem can vary from the transport of the prompt radiation to the transport, during the cooling, of the residual one. In the latter case, the concrete blocks that in the roof of the dump casemate are removable have also been also removed in the simulation during the cooling time, and replaced with air.

The FLUKA model used in the case of the copper beam dump is shown in Figure 14. The two usual irradiation patterns have been studied, for short- and long-term irradiations. The results for the two beam dump models are reported in Figures 15 and 16. In the case of the beam dump in copper, the H*(10) rate due to the residual radiation over the roof is at the level of 1 Sv/h after the 24-hour cooling that follows or follow 24-hour irradiation. This very high value definitely requires a better protection against the dose from activation, to make the area over the roof accessible for the maintenance, even with the opportune restrictions. This better protection could come from additional local shielding – for example with concrete slabs – around the copper structure in the dump casemate. In the case of the bi-material dump the H*(10) over the roof due to the activated materials in the dump is at the level of 10 mSv/h after the 24 hours of cooling that follows the short-term irradiation. This value, which is already two orders of magnitude lower with respect to the previous case, can be lowered further by using a proper shielding against the radiation coming from the activation: experience at high-energy accelerators shows, for example, that quite narrow slabs of marble around the dumps are highly effective[1]. The picture of the residual H*(10) rate 30 days after the long-term irradiation, moreover, shows how well, with this beam dump choice, the residual radiation is contained in the inner part of the dump, allowing the access to the roof.

As a last step, a study of the residual specific activity in the dump materials has been done. In Figure 17 the residual specific activities in the carbon core and in the "hottest" part of the stainless steel are reported for the bi-material dump, after a long-term irradiation and for a cooling time of 30 days. The total specific activity for the stainless steel is at the level of $10^9$ $Bq/cm^3$, while in the carbon core is around $10^3$ $Bq/cm^3$.

[1] A. Fasso private communication.

**Figure 14: FLUKA model of the copper beam dump**

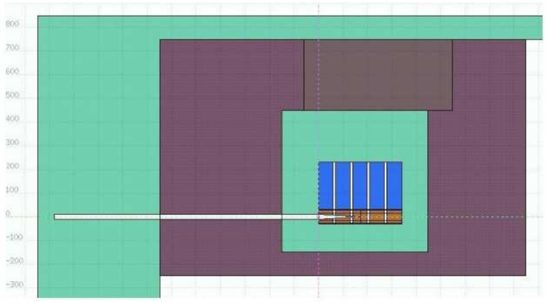

The concrete cage around the beam dump is described, with the last meters of the beam-line and, on the roof, the concrete blocks that are removable when the accelerator is not in operation.

**Figure 15: Residual H*(10) rate (in mSv/h) in the concrete cage and over the cage roof in the case of the dump in copper, for two typical cooling times after a short-and a long-term irradiation**

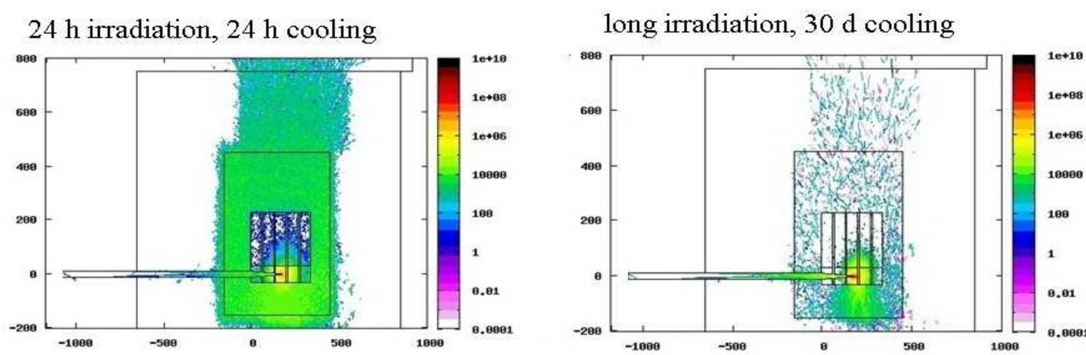


**Figure 16: Residual H*(10) rate (in mSv/h) in the concrete cage and over the cage roof in the case of the bi-material dump, 24 hours after a 24 hours irradiation and 30 days after a long-term irradiation**

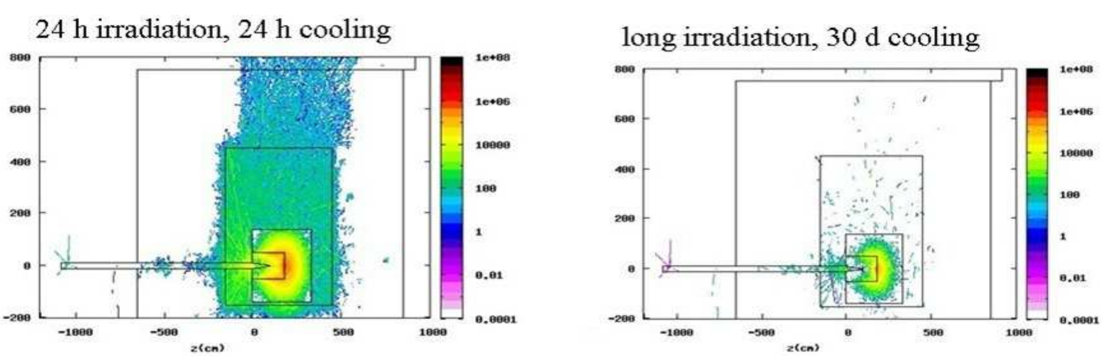

**Figure 17: Specific residual activity of the carbon core and the stainless steel "hottest" part in the case of the bi-material dump, after a long-term irradiation and a cooling time of 30 days**

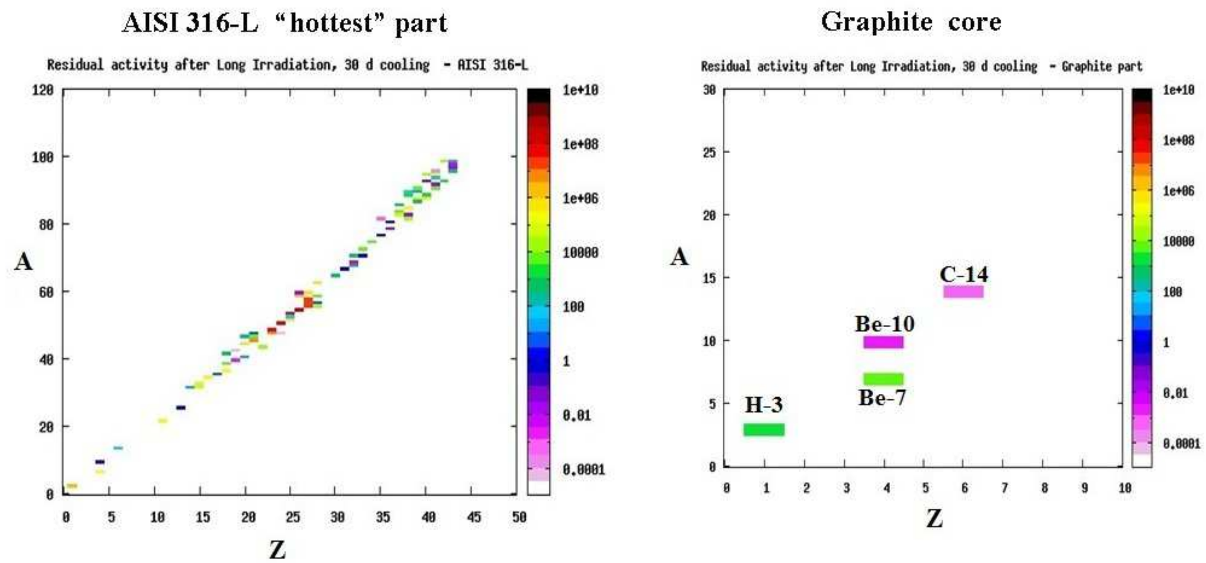


In the Z-A plane the main radionuclides that contribute to the activity are shown.

In the case of the copper dump the results for the "hot" part of the dump are those of the left sides of Figures 7 and 8: it can be observed that a value of 1.2 $10^{10}$ Bq/cm$^3$ is still present at the end of the 10 years of cooling that follows the long-term irradiation.

## Residual dose rates due to the beam losses along the beam-line

Beam losses along the beam-line have to be minimised to keep activation at an acceptable level for hands-on maintenance and to protect equipment. Operational results from the Spallation Neutron Source at ORNL show that an uncontrolled beam loss level of about 1 W/m is fully consistent with a hands-on maintenance philosophy [10]. To check the validity of this assumption in the case of MYRRHA, an additional Monte Carlo study with the FLUKA code has been performed. The last 100 meters of the LINAC horizontal tunnel have been simulated, including the pipe of the beam-line in stainless steel and 10 collimators in copper, one every 10 m. The concrete walls along the tunnel have been also included and described with the first 30 cm of their thickness, in order to take into account the backscattered component of the neutron radiation. A continuous beam loss of 1 nA/m has been then assumed and a continuous, linear distributed proton source corresponding to this loss has been described. In order to take into account the realistic behaviour of the proton beam, the proton energy has been described in the model as linearly increasing along the line. The two irradiation patterns studied in the analysis in the previous sections have been assumed, for short-and long-term irradiations. In the case of the short-term (24 h) irradiation the initial residual dose rate of about 200 μSv/h at EOI at the distance of 1 m goes down, after the first 24 hours cooling, to ~ 10-30 μSv/h, depending on the position along the line. Therefore, a human intervention on the line seems possible in a reasonable time after the end of the irradiation. After a long-term irradiation and the first 30 days cooling the ambient dose equivalent residual rate varies from few up to ~ 50 μSv/h, still a limited value, which seems low enough to allow a human intervention.

In addition to these simulations, a second study has been performed with the aim of evaluating the radiological impact of eventual "hot spot losses" of 100 nA due to the collimators. Figure 18 shows the results of this simulation for a short-term irradiation. In the top picture, which shows the behaviour of the residual H*(10) rate at EOI, the effect of the collimators and the effect of the increasing proton energy are clearly visible. The high dose rate of few mSv/h at the end of the short-term irradiation goes down to values between 100 μSv/h up to several hundreds μSv/h after 24 hours. A similar result, which should be seen as a superior limit due to the pessimistic value of the assumed "hot spot" losses, would require a longer waiting time before an eventual access close to the line.

**Figure 18: Residual H*(10) rates (in μSv/h) around the last 100 m of the horizontal beamline, for two representative cooling times (EOI and 24 h) after a 24 h irradiation, with the hypothesis (100 nA) of hotspot losses due to the collimators**

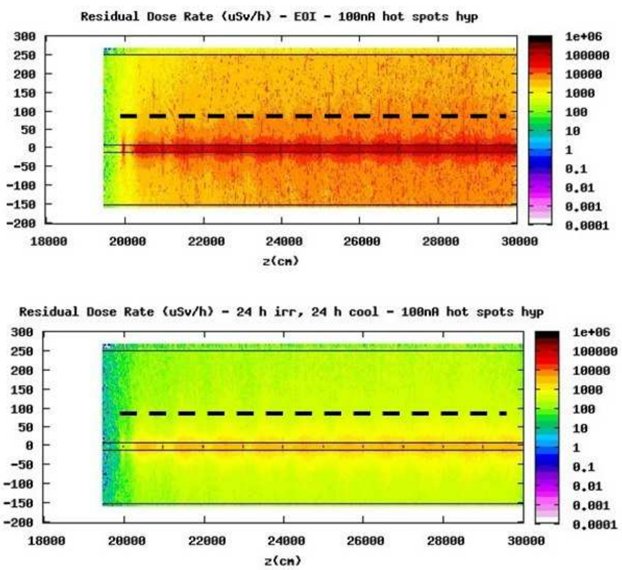


## Conclusions

Firstly, a general Monte Carlo study has been presented, with the aim of optimising some aspects of the shielding of the MYRRHA proton beamline, as well as quantifying the activation problems that heavily influence the design. Results about neutron double differential yields and induced radioactivity from irradiated thick samples of carbon, aluminium, iron, stainless steel and copper are intended to be a simple database, to address the choice of the main structural materials. The optimisation study of the beam dump showed that, besides a first design of a beam dump in copper, a beam dump solution with a soft, low Z material for the core, surrounded by a medium-high Z material is optimal under the point of view of the induced activation, improving the accessibility and the long-term treatment of the irradiated elements. Detailed thermal and mechanical studies will be needed to better assess the feasibility of all the proposed solutions.

## Acknowledgements

The research leading to these results has received funding from the European Atomic Energy Community Seventh Framework Programme (FP7/2007-2013) under Grant Agreement no 232527.

## References


[1] D. De Bruyn, H. Aït Abderrahim, P. Baeten, R. Fernandez (2011), MYRRHA, the Multi-purpose Hybrid Research Reactor for High-tech applications, Proc. of the International Congress on Advances in NPPs (ICAPP '11), Nice, France 2-6 May 2011, France Omnipress, 472-478.

[2] N.V. Mokhov (2010), Dealing with MegaWatt beams, *Proc. of the SATIF-10 Workshop,* CERN 2-4 June 2010, OECD/NEA publication 6898, 105-111.

[3] A. Ferrari, S. DiMaria, M. Sarotto, A. Stankovskiy (2012), Shielding and activation calculations for the MYRRHA ADS design in the sub-critical operation mode, *ICRS12 Conference*, Nara, Japan 2-7 September 2012.

[4] A. Ferrari, P. Sala, A. Fassò, J.Ranft (2005), FLUKA: A multi-particle transport code, CERN-2005-10, INFN/TC_05/11, SLAC-R-773.

[5] G. Battistoni *et al.* (2007), The FLUKA code: description and benchmarking, *Proceedings of the Hadronic Shower Simulation Workshop 2006,* Fermilab 6-8 September 2006, AIP Conference Proceedings, 896, 31-49 (2007).

[6] F. Cerutti, N. Charitonidis, M. Silari (2010), Neutron double differential distributions, dose rates and specific activities from accelerator components irradiated by 50-400 MeV protons, *Proc. of the SATIF-10 Workshop,* CERN 2-4 June 2010, OECD/NEA publication 6898, 139-155.

[7] http://aea.web.psi.ch/Urs_Rohrer/MyWeb/pkanal.htm.

[8] A. Ferrari, T. Cowan, D. Margarone, J. Prokupek, B. Rus (2010), Shielding assessment for the ELI high-intensity laser beamline facility in the Czech Republic, *Proc. of the SATIF-10 Workshop,* CERN, 2-4 June 2010, OECD/NEA publication 6898, 105-111.

[9] A. Ferrari, E. Amato, D. Margarone, T. Cowan, G. Korn (2012), Radiation field characterization and shielding studies for the ELI Beamlines Facility, Applied Surface Science, http://dx.doi.org/10.1016/j.apsusc.2012.09.105.

[10] J. Galambos (2008), Operational experience with high power beams at the SNS superconducting LINAC, *Proc. of the LINAC2008 Conference,* Victoria, Canada.